Bull. Mater. Sci., Vol. 37, No. 5, August 2014, pp. 1147–1152. © Indian Academy of Sciences.

X-ray peak broadening analysis of $Fe_{50}Ni_{50}$ nanocrystalline alloys prepared under different milling times and BPR using size strain plot (SSP) method

L HOSSEINZADEH[a], J BAEDI[a] and A KHORSAND ZAK[b,*]

[a]Deaprtment of Physics, Hakim Sabzevari University, Sbzevar 9617976487, Khorasan Razavi, Iran
[b]Nanotechnology Laboratory, Esfarayen University of Technology, Esfarayen 9661998195, North Khorasan, Iran

MS received 22 July 2013; revised 28 October 2013

Abstract. **$Fe_{50}Ni_{50}$ nanocrystalline alloys were prepared by mechanical alloying method at different milling times of 2, 5, 10, 30, 50 and 70 h and ball powder ratios (BPR) of 10 : 1, 20 : 1 and 30 : 1. The structures of prepared powders were studied by X-ray diffraction (XRD). The broadening of the diffraction peaks were analysed using size strain plot (SSP) method and the lattice strain and crystallite size of the nanocrystals were calculated. In addition, the typical morphological studies were performed by scanning electron and transmission electron microscopies (SEM and TEM). The results showed that the crystallite size of the nanocrystals decreased with the milling time and BPR increases; whereas, the lattice constant (*a*) increased. Vibrating sample magnetometer (VSM) study of the powder prepared at 50 h and BPR 30 : 1 showed that the sample exhibits both the superparamagnetic and ferromagnetic properties in nanocrystallite size range.**

Keywords. **Fe–Ni; peak broadening; X-ray diffraction; ball milling.**

1. Introduction

Soft magnetic materials are used extensively in electromotors as voltage and current transformers, saturable reactors, magnetic amplifiers, inductors and chokes (Zhang 1997; Saravanan *et al* 2001; Yoshizawa 2001; Lee *et al* 2004, 2012; Ma *et al* 2006; Zheng *et al* 2009; Yildiz *et al* 2013). Fe–Ni alloy known as a typical soft magnetic material exhibits attractive magnetic properties. $Fe_{20}Ni_{80}$ alloys exhibit the highest known permeability of 95,000 with a coercive force of only 0·02 A cm^{-1} for synthesized soft magnetic materials. $Fe_{50}Ni_{50}$ has a higher coercive force and saturation magnetic induction when compared to $Fe_{20}Ni_{80}$ for the same excitation field (Bas *et al* 2003), whereas $Fe_{70}Ni_{30}$ shows a higher electrical resistivity (Liu *et al* 2005). Therefore, very high permeability and very low coercive force of Fe–Ni alloys make them suitable for use in circuits that are excited by very low currents and require quick response. Nanostractured materials show interesting properties due to finite size. Therefore, several chemical and physical methods have been designed to prepare Fe–Ni nanocrystalline materials such as electroless chemical reduction, rapid sintering nanotemplate approach (Kim *et al* 2007; Moustafa and Daoush 2007; Lee *et al* 2012). Among these methods, mechanical activation like high-energy ball milling of crystalline solids provides a way for the synthesis of nanostructured materials, amorphous alloys and quasicrystalline phases (Menzel *et al* 2001; Suryanarayana 2001). Mechanical alloying (MA) is a solid-state powder processing technique involving repeated fracturing, welding and re-welding of powder particles in a high-energy ball mill system. MA has been used for synthesizing a variety of equilibrium and non-equilibrium alloy phases starting from blended elemental or pre-alloyed powders (Suryanarayana 2001). Milling time length is one of the important parameters in milling operation. Usually, the time length chosen for milling operation is the one in which a balance state is created between fracturing and cold welding in particle powders. The time required is different based on the following parameters, from which, type and speed of milling, ratio of ball to powder and temperature are mentioned. In this work, $Fe_{50}Ni_{50}$ nanocrystals were prepared by high-energy ball milling technique using powder of pure crystallite metals as starting materials and toluene was used as a process control agent (PCA). Different alloying times and ratio of ball to powder (BPR) were considered. The structural properties and XRD peak broadening of the prepared materials were investigated by SSP method to evaluate the crystallite sizes and lattice strains.

2. Experimental

2.1 *Materials and methods*

High purity Fe and Ni powders (99·5 and 99·98%, respectively, from Sigma-Aldrich) were used to synthesize

*Author for correspondence (alikhorsandzak@gmail.com)

$Fe_{50}Ni_{50}$ nanocrystallite alloy by a commercial Fritsch Pulverisette 5 planetary ball-mill mechanical alloying machine. Eight samples with the molar combination of 50–50 were prepared. It is necessary to use a process control agent (PCA) to prevent agglomeration of the powders (Pei-Heng *et al* 2005). For this propose, toluene was used as a PCA in this research. In addition, to prevent oxidation of the mixed powder during the milling process, the mixed powders were sealed in a 125 mL cylindrical vial containing stainless steel balls (d = 10 mm) inside a glove box with argon atmosphere. The alloying times of 2, 5, 10, 30, 50 and 70 h and BPR of 10 : 1, 20 : 1 and 30 : 1 are chosen for ball-milling process of the eight samples. Vial rotation speed was fixed at 300 rpm for all the samples. To avoid excessive heating during milling, each 1 h of milling process was followed by a stay during 10 min under the argon atmosphere at room temperature.

2.2 *Instrumental*

X-ray diffraction patterns were recorded using D8, Bruker. Field emission scanning electron and transmission electron microscopies (FESEM and TEM, Hitachi) have been used for morphology and microstructure observations. For providing these images, very little amount of milled powder poured on carbon glue which is connected to sample vessel, so that powder particles would not pile on each other.

3. Results and discussion

3.1 *X-ray diffraction studies*

Figure 1(a) shows the evolution of X-ray diffraction patterns of the prepared $Fe_{50}Ni_{50}$ nanocrystal powders under BPR 30 : 1 and different milling times of 2, 5, 10, 30, 50 and 70 h. It is clearly observed that the FWHM of the (111) peak increases with increase in the milling time as crystallite size decreases. XRD pattern of the sample milled for 2 h shows reflections corresponding to body-centered-cubic (BCC) Fe (*Im*-3*m*, ref. code: 00-006-0696) and face-centered-cubic (*fcc*) Ni (*Fm*-3*m*, ref. code: 00-001-1258) metals. In addition, the crystallite size of the prepared powders are definitely smaller for Fe and Ni pure powders, figure 1(b). It shows that the bonds between Fe and Ni atoms are broken during the milling process, resulting to smaller crystallite size product. For all of the samples milled for more than 2 h, $Fe_{50}Ni_{50}$ solid solutions (*Fm*-3*m* space groups, ref. code: 0-003-1209) are formed with broader diffraction peaks and therefore, smaller crystallite sizes are obtained. Figure 2 shows X-ray diffraction patterns of $Fe_{50}Ni_{50}$ nanocrystallite powders prepared by ball-milling method with different BPR (10 : 1, 20 : 1 and 30 : 1) at alloying times of 50 h. As expected, FWHM of the diffraction peaks are broadened with increasing BPR. This suggests a continuous decrease of the crystallite size. Smaller crystallite size results in the increase of grain boundaries, which in return increases surface/volume ratio and therefore, there will be more atoms on the surface. Furthermore, free bonds between atoms increase and lower average force will be experienced by an atom from the other atoms, which will result in the increase of the lattice constant in smaller grains.

3.1a *Evaluation of the crystallite size and mechanical properties*: The crystallite size and lattice strain of the $Fe_{50}Ni_{50}$ nanocrystals prepared at different milling times of 2, 5, 10, 30, 50 and 70 h and different BPR of 10 : 1, 20 : 1 and 30 : 1 (milled for 50 h) were calculated by size–strain plot method (SSP). Normally, the crystallite size of the crystals are determined by X-ray line broadening method using the Scherrer equation

$$D = (k\lambda/\beta\cos\theta),$$

where D is the crystallite size, λ the wavelength of the radiation (1·54056 Å for CuKα radiation), k a constant equal to 0·94, β the peak width at half-maximum intensity (FWHM) and θ the peak position. The breadth of the Bragg peak is a combination of both instrument- and sample-dependent effects (Khorsand Zak *et al* 2011). To decouple these contributions, it is necessary to collect a diffraction pattern from the line broadening of a standard material (e.g. silicon) to determine the instrumental broadening. The instrument-corrected broadening, β_D corresponding to the diffraction peak of the samples were estimated using the relation

$$\beta_D^2 = [(\beta^2)_{\text{measured}} - (\beta^2)_{\text{instrument}}] \Rightarrow D = \frac{k\lambda}{\beta_D \cos\theta}.$$

According to our previous works, line broadening was essentially isotropic using the Williamson–Hall method (Khorsand Zak and Abd. Majid 2010; Khorsand Zak *et al* 2011), indicating that the diffracting domains were isotropic and a micro-strain contribution also occurred. However, in the cases of isotropic line broadening, a better evaluation of the size–strain parameters can be obtained by considering an average size–strain plot (SSP), which gives less weight to data from reflections at high angles, where the precision is usually lower. In this approximation, it is assumed that the crystallite size profile is described by a Lorentzian function and that the strain profile is described by a Gaussian function (Khorrami *et al* 2012; Khorsand Zak *et al* 2012a, b). Furthermore, the peak broadening that occurred due to the strain is estimated from $\varepsilon \approx \beta_s/\tan\theta$ (Cullity 1956). The total peak broadening is obtained from the following equation

$$\beta_{hkl} = \beta_s + \beta_D.$$

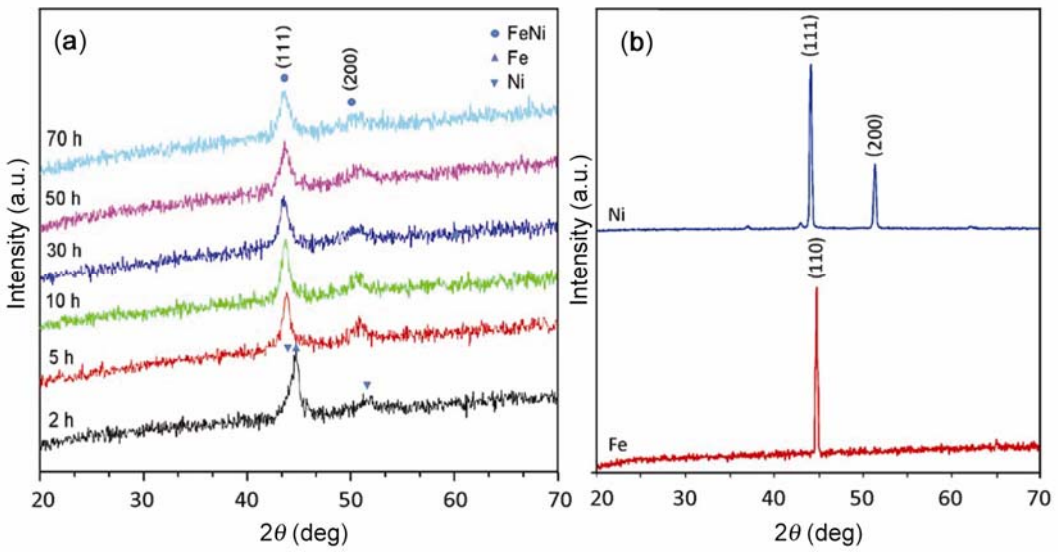

Figure 1. (**a**) X-ray diffraction patterns of $Fe_{50}Ni_{50}$ nanocrystalline powders prepared at different milling times of 2, 5, 10, 30, 50 and 70 h with BPR of 30 : 1. (**b**) X-ray diffraction of the pure Fe and Ni powders.

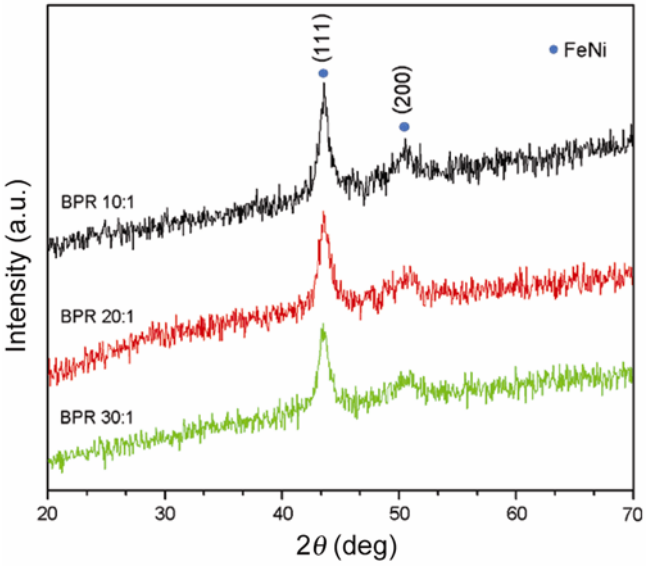

Figure 2. X-ray diffraction patterns of $Fe_{50}Ni_{50}$ nanocrystalline powders prepared at milling time of 50 h under different BPR of 10 : 1, 20 : 1 and 30 : 1.

Therefore, we obtain

$$(d_{hkl}\beta_{hkl}\cos\theta)^2 = \frac{A}{D}(d_{hkl}^2\beta_{hkl}\cos\theta) + \left(\frac{\varepsilon}{2}\right)^2,$$

where A is a constant that depends on the shape of the particles; for spherical particles, it is given as approximately 3/4 and can be used for the samples. In figure 3(a and b), the term $(d_{hkl}\beta_{hkl}\cos\theta)^2$ is plotted with respect to $(d_{hkl}{}^2\beta_{hkl}\cos\theta)$ for both orientation peaks of $Fe_{50}Ni_{50}$ nanoparticles from $2\theta = 20°$ to 70° for samples prepared at different milling times and different BPR, respectively. In this case, the crystallite size is determined from the slope of the linearly fit data, where the root of the y-intercept gives the strain. Figure 4(a) shows the average crystallite size of $Fe_{50}Ni_{50}$ vs milling time and their corresponding strain lattice values. As can be seen, at the early stage of milling, the crystallite size increases rapidly, but decreased with increase in the milling time with a final value of about 16·30 nm. This crystallite size value is smaller than that reported for $Fe_{50}Ni_{50}$ nanocrystals synthesized via gas-condensation method (Scorzelli *et al* 1986; Djekoun *et al* 2004). Figure 4(b) presents the variation of the crystallite size of $Fe_{50}Ni_{50}$ samples milled for 50 h vs BPR (10 : 1, 20 : 1 and 30 : 1). It can be seen that the value of crystallite size of $Fe_{50}Ni_{50}$ decreased when BPR increases due to effective encounter between materials and balls. The lattice constant of the samples as a function of milling time and BPR are shown in figure 5. It is clearly observed that the lattice constant increases with the crystallite size increase. As mentioned earlier, decrease in crystallite size resulted to lower average inner force in the lattice, which results in the increase of the lattice constant (a).

3.2 *Morphology analysis*

Powder morphologies were studied by SEM imaging. Figure 6(a–d) shows the morphological evaluation of $Fe_{50}Ni_{50}$ alloy prepared with BPR 30 : 1 and milling times of 30, 50 and 70 h. Figure 6(d and e) shows TEM morphology of the sample prepared at 50 h with BPR 30 : 1 attached to its corresponding EDX, respectively. It is clearly seen that the powders contain small particles that agglomerated together in bigger particles. These agglomerated particles are separated and dispersed in

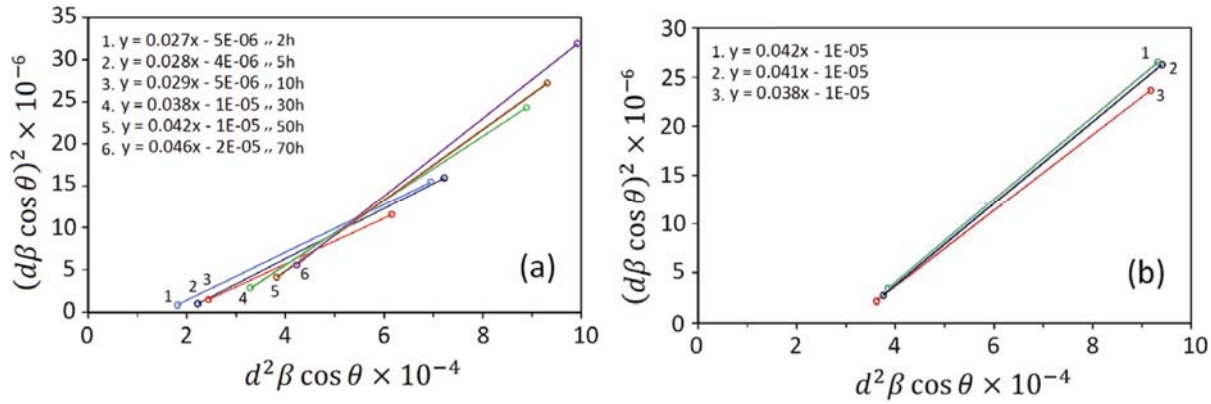

Figure 3. Size–strain plot of $Fe_{50}Ni_{50}$ nanocrystalline powders prepared at (**a**) different milling time and (**b**) under different BPR.

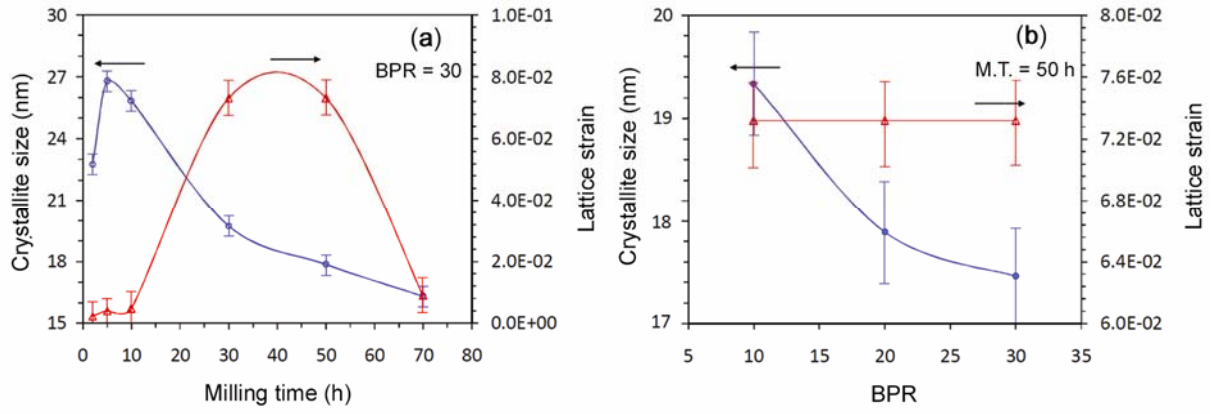

Figure 4. Variation of crystallite size and lattice strain for $Fe_{50}Ni_{50}$ nanocrystalline powders prepared (**a**) at different milling times and (**b**) under different BPR.

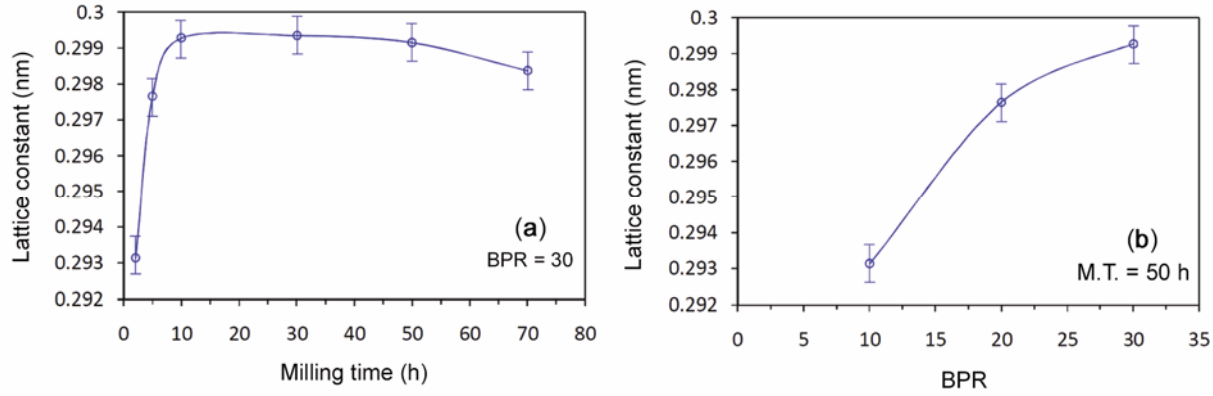

Figure 5. Variation of lattice constant for $Fe_{50}Ni_{50}$ nanocrystalline powders prepared (**a**) at different milling times and (**b**) under different BPR.

ethanol solution using ultrasonication process and then dropped on a silicon substrate for SEM imaging. The insets of SEM images show the higher magnification SEM images of the prepared particles in scale of 500 nm. These images confirm that the sizes of the particles are in nanorange, which is confirmed with TEM images. In addition, the sizes of the agglomerate particles are decreased by increasing the milling time from 30 to 70 h.

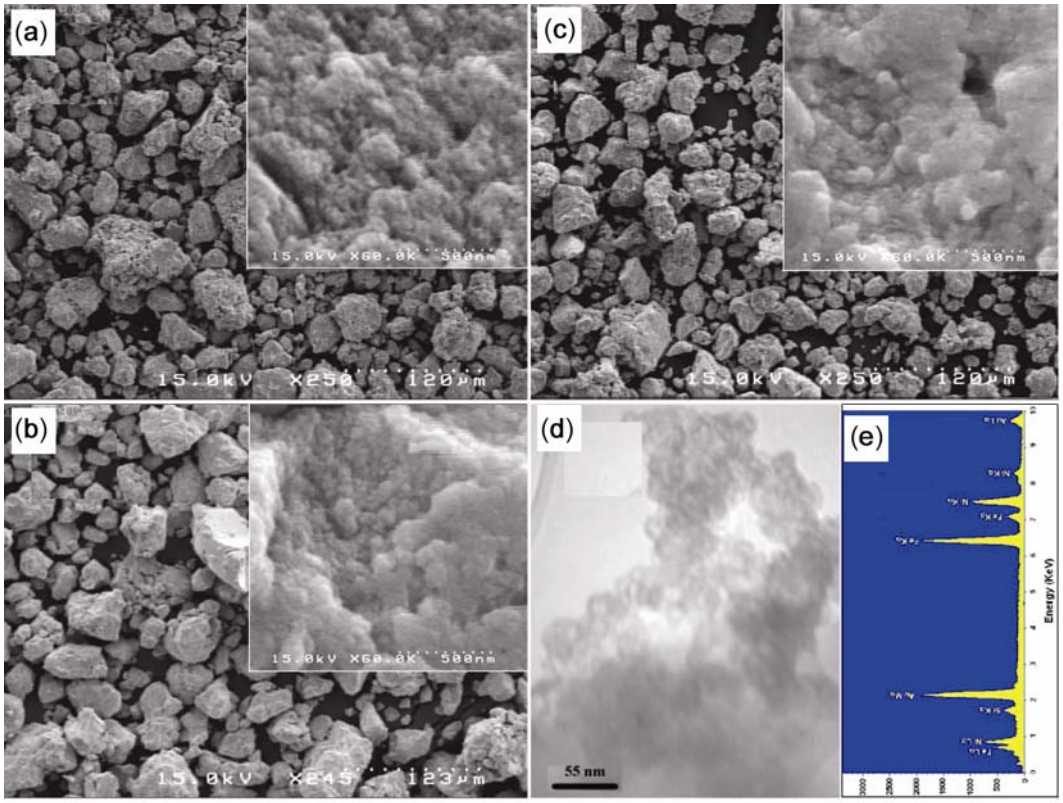

Figure 6. (**a**–**c**) SEM micrograph of $Fe_{50}Ni_{50}$ nanocrystalline powders prepared (a) at different milling times of 30, 50 and 70 h. (**d** and **e**) TEM image of $Fe_{50}Ni_{50}$ nanocrystalline powders prepared at milling time of 50 h under BPR of 30 : 1 and its corresponding EDX, respectively.

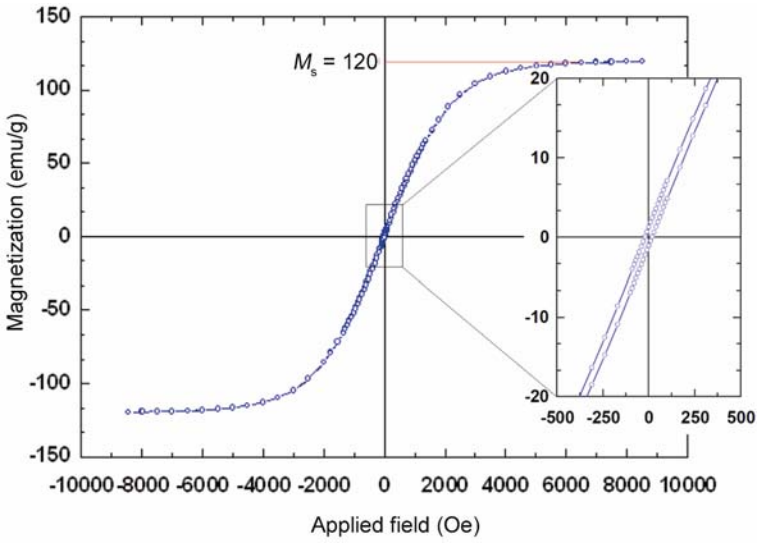

Figure 7. VSM graph of $Fe_{50}Ni_{50}$ nanocrystalline powders prepared at milling time of 50 h under BPR 30 : 1.

The EDX carried out on the sample prepared at 50 h with BPR 30 : 1, figure 6(d). The elements of Fe, Ni and Au are detected in the EDX spectrum. Existence of Au is related to the gold-coating process of sample before SEM imaging.

3.3 *Vibrating sample magnetometer analysis*

Figure 7 shows an example of hysteresis curve (M vs H) for sample milled for 50 h. By looking at the image, a saturation magnetization (M_s) of 120 emu/g is obtained

for the sample. Guittoum and co-workers (2008) showed that the M_s is decreased with increasing the milling time due to decreasing of the crystallite size. Also, it is well known that iron and nickel show ferromagnetism behaviour. But supermagnetism behaviour was found in $Fe_{50}Ni_{50}$ alloy. This behaviour is related to the small crystallite size of the sample (Sorensen 2001). There is a size limit, which small particles can no longer gain a favourable energy configuration, because of the formation of domains costs energy due to wall formation. For a particle size, D, the magnetostatic energy is equal to $M_s^2D^3$. For a critical size or single domain size, D_s, below which a particle will not form a domain. Then, we have $D_s \approx \gamma/M_s^2$. Here γ is the domain wall energy per unit area. The amount of D_s for Fe and Ni particles were obtained to be 14 and 55 nm, respectively (Leslie-Pelecky and Rieke 1996). If we look at the enlarged part of the hysteresis curve in figure 7, it can be seen that the sample shows small ferromagnetism beside the superparamagnetism behaviour. It is due to the existence of the particles bigger than 15 nm in the synthesized powder. These results are in good agreement with the results obtained from SEM and TEM images.

4. Conclusions

The $Fe_{50}Ni_{50}$ nanocrytalline powders were prepared by a mechanical alloying method. The effect of milling time (2, 5, 10, 30, 50 and 70 h) and BPR (10 : 1, 20 : 1 and 30 : 1) on the XRD peak broadening, crystallite size and lattice strain were investigated. The crystallite size of the samples prepared at different milling times of 2, 5, 10, 30, 50 and 70 h and different BPR of 10 : 1, 20 : 1 and 30 : 1 were obtained to be 27·78, 26·79, 25·89, 19·74, 17·86, 16·30 nm and 19·74, 18·29 and 17·89 nm, respectively. Typical morphological studies were carried out on the samples prepared at milling times of 30, 50 and 70 h and particle size of the samples were observed to be less than 50 nm. Finally, VSM study of the sample, which prepared at milling time of 50 h with BPR of 30 : 1 showed both superpara- and ferro-magnetic properties due to the small particle size.

References

Bas J A, Calero J A and Dougan M J 2003 *J. Magn. Magn. Mater.* **254–255** 391

Cullity B D 1956 *Elements of X-ray diffraction* (California: Addison–Wesley Publishing Company Inc)

Djekoun A, Bouzabata B, Otmani A and Greneche J 2004 *Catal. Today* **89** 319

Guittoum A, Layadi A, Bourzami A, Tafat H, Souami N, Boutarfaia S and Lacour D 2008 *J. Magn. Magn. Mater.* **320** 1385

Khorrami G H, Khorsand Zak A, Kompany A and Yousefi R 2012 *Ceram. Int.* **38** 5683

Khorsand Zak A and Abd. Majid W H 2010 *Ceram. Int.* **36** 1905

Khorsand Zak A, Abd. Majid W H, Abrishami M E and Yousefi R 2011 *Solid State Sci.* **13** 251

Khorsand Zak A, Majid W H A, Ebrahimizadeh Abrishami M, Yousefi R and Parvizi R 2012a *Solid State Sci.* **14** 488

Khorsand Zak A, Yousefi R, Majid W H A and Muhamad M R 2012b *Ceram. Int.* **38** 2059

Kim J H, Kim J, Lim S K, Kim C K and Yoon C S 2007 *J. Magn. Magn. Mater.* **310** 2402

Lee J-S, Kang Y-S, Kwon S-K, Cha B-H and Qin X 2004 *Adv. Powder Technol.* **15** 639

Lee Y-I, Lee J-T and Choa Y-H 2012 *Ceram. Int.* **38** 4305

Leslie-Pelecky D L and Rieke R D 1996 *Chem. Mater.* **8** 1770

Liu Y, Zhang J, Yu L, Jia G, Jing C and Cao S 2005 *J. Magn. Magn. Mater.* **285** 138

Ma Y, Xiao L and Yan L 2006 *Chin. Sci. Bull.* **51** 2944

Menzel M, Šepelák V and Becker K D 2001 *Solid State Ionics* **141–142** 663

Moustafa S F and Daoush W M 2007 *J. Mater. Proc. Technol.* **181** 59

Pei-Heng Z, Long-Jiang D, Jian-Liang X, Di-Fei L and Liand C 2005 *J. Electron. Sci. Technol. China* **3** 164

Saravanan P, Jose T A, Thomas P J and Kulkarni G U 2001 *Bull. Mater. Sci.* **24** 515

Scorzelli R B, Danon J and Da Silva E G 1986 *Hyperfine Interactions* **28** 979

Sorensen C M 2001 In *Nanoscale materials in chemistry* (ed) K J Klabunde (New York: John Wiley & Sons, Inc)

Suryanarayana C 2001 *Prog. Mater. Sci.* **46** 1

Yildiz G, Yildiz Y and Nezir S 2013 *Bull. Mater. Sci.* **36** 93

Yoshizawa Y 2001 *Scr. Mater.* **44** 1321

Zhang Y 1997 *Chin. Sci. Bull.* **42** 1218

Zheng Y, Tong C, Wang B, Xie Y, Liao H, Li D and Liu X 2009 *Chin. Sci. Bull.* **54** 2998